Journal of Energy and Power Engineering 11 (2017) 363-371
doi: 10.17265/1934-8975/2017.06.001

Rocket Propulsion Powered Using a Gyrotron

Masafumi Fukunari[1], Kimiya Komurasaki[2], Yusuke Nakamura[3], Yasuhisa Oda[4] and Keishi Sakamoto[4]

1. Research Center for Development of Far-Infrared Region, University of Fukui, Fukui 910-8507, Japan

2. Department of Aeronautics & Astronautics, University of Tokyo, Bunkyo, Tokyo 113-8656, Japan

3. Graduate School of Frontier Sciences, University of Tokyo, Kashiwa, Chiba 277-8561, Japan

4. National Institutes for Quantum and Radiological Science and Technology, Naka, Ibaraki 311-0193, Japan

Received: April 28, 2017 / Accepted: May 10, 2017 / Published: June 30, 2017.

Abstract: This paper presents a review of a beamed energy propulsion rocket, the Microwave Rocket, which produces propulsive thrust from millimeter-wave beams transferred from the ground. The thrust is generated through millimeter-wave discharge driven in a cylindrical thruster. As a high-power millimeter-wave generator, a Gyrotron is promising as the beam source. The salient benefit of Microwave Rockets is the resultant drastic cost reduction of mass transportation into space. We have already conducted launch experiments and have achieved continuous thrust generation under multi-pulse operation. Recently, a long-distance beam transfer system has been developed. Ignition tests have been conducted. The physics of the millimeter-wave discharge remain unclear. Additional studies using experimentation and calculations must be conducted to optimize the thrust generation.

Key words: Beamed energy propulsion, microwave discharge, wireless power transfer, gyrotron.

Acronyms/Abbreviations

MSD	Microwave supported detonation
LSD	Laser supported detonation
WPT	Wireless power transfer
BEP	Beamed energy propulsion
QST	National Institutes for Quantum and radiological Science and Technology
C-J	Chapman-Jouguet
CFD	Computational fluid dynamics

1. Introduction

In conventional cars and spacecraft, fuel is always kept on-board. Accordingly, it must increase concomitantly with increased load mass, velocity increment, and travel distance. Actually, fuel is necessary to move the fuel itself. Therefore, the payload ratio is limited. For example, assuming that a chemical rocket is launched into geostationary earth orbit, the payload mass is only 1% of the total mass, at maximum. The WPT, which transfers energy by an electromagnetic-wave beam, can be a promising solution to the tradeoff relation. The WPT propulsion rocket concept, called the BEP launcher, was proposed by Kantrowitz in 1972 [1]. Many studies of BEP launchers have been conducted using laser or microwave beams [2-4].

The Microwave Rocket is a BEP launcher using a megawatt class millimeter-wave oscillator Gyrotron. The Gyrotron, developed as a heating device for nuclear fusion plasma, has already achieved high-power, long-pulse, high-efficiency operation such as 1 MW/800 s/55% electrical efficiency at the National Institutes for Quantum and Radiological Science and Technology (QST/JAEA) [5]. Generally, “microwaves” are 3-30 GHz electromagnetic waves; the 30-300 GHz frequency band is called “millimeter-wave”. However, in the field of BEP, the frequency bands are often categorized only as laser or microwave. Moreover, “microwave” has higher name recognizability than “millimeter wave” does. These are reasons why we have designated the BEP launcher as a Microwave Rocket.

Corresponding author: Masafumi Fukunari, Ph.D., specially appointed assistant professor, research fields: millimeter wave, millimeter wave discharge, gyrotron, beamed energy propulsion.

Microwave Rockets can drastically reduce mass transportation costs to space. The bottleneck hindering space exploration is the huge transportation cost attributable to chemical rockets. Conventional rockets require huge amounts of fuel and propellant. The fuel consumption is determined by the exhaust velocity (specific impulse), which is accordingly limited by the chemical energy per unit mass of fuel. The fuel consumption of the current rocket has already reached the theoretical limits. Microwave Rockets do not have the limitation because the energy source is separate from the rocket. Furthermore, Microwave Rockets can use atmospheric air as a propellant by using an air-breathing system. In such cases, no on-board propellant is needed. The payload ratio can be much higher than those of chemical rockets. Furthermore, the Microwave Rocket engine structure is theoretically simple because the thruster acquires high pressure by shock wave compression using the MSD without a complex and expensive turbo-pump system. Consequently, the manufacturing cost can be low. Ground facilities include a substantial number of gyrotron and energy storage facilities. Although the construction cost is dominant in all costs, the costs can be amortized by repeated launches.

Experimental studies of Microwave Rockets have been conducted using a megawatt class gyrotron at the National Institutes for Quantum and radiological Science and Technology (QST). Numerical studies of millimeter wave discharge have been conducted to investigate ionization mechanisms. As described herein, we describe the thrust generation process, a launch demonstration of the rocket, and numerical computation of millimeter wave discharge as a review of Microwave Rocket studies.

2. Thrust Generation Processes Using MSD

Fig. 1 presents the thrust generation process. The thruster is a cylindrical tube with one side closed. A parabolic mirror is mounted at the closed end as an ignitor. The parabolic mirror focuses the incident beam. Then the discharge is ignited at the focal point. A screw is often set at the focal point to support the ignition in experiments using a model rocket. The ionization front of the discharge propagates toward the beam source, absorbing the millimeter-wave energy. A shock wave is driven by the discharge. High pressure behind the shock wave imparts the thrust impulse to the thruster. Impulsive thrust I_{th} is determined by the time integral of the pressure p_w at the closed end during engine cycle time τ.

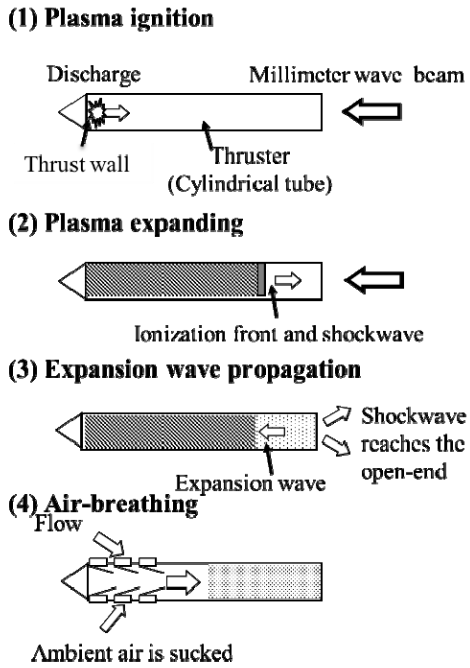

Fig. 1 Thrust generation process.

$$I_{\mathrm{th}} = A_w \int_0^{\tau} p_w dt \quad (1)$$

Consequently, the closed end is called the thrust wall. A_w represents the area of the thrust wall. The ratio of the I_{th} on the incident energy is called the momentum coupling coefficient C_{m}, which is equal to the ratio of the time averaged thrust $\bar{F}_{\mathrm{th}}$ on average power P_{av}.

$$C_{\mathrm{m}} = \frac{I_{\mathrm{th}}}{P_{\mathrm{b}} t_{\mathrm{pls}}} = \frac{\bar{F}_{\mathrm{th}}}{P_{\mathrm{av}}} \quad (2)$$

In Eq. (2), P_{b} denotes the peak power; t_{pls} is the pulse duration. The BEP launcher thrust performance is usually evaluated by C_{m}.

The phenomenon is called MSD by analogy with chemical detonation. When the MSD arrives at the open end, the beam must be cut off to avoid energy loss. An expansion wave then starts to propagate from the open end to the thrust wall. The pressure at the thrust wall is maintained as high until the expansion wave reaches the thrust wall and the thruster acquires an impulsive thrust. Negative gauge pressure is then generated at the thrust wall because of the reflection of the expansion wave. An air-breathing system such as a reed valve mounted at thruster side wall refreshes the inside gas. The Microwave Rocket is accelerated, repeating this engine cycle.

3. Launch Experiments

Launch experiments have been conducted with a gyrotron in QST. The first launch experiment was conducted in 2003 by 930 kW single pulse operation. Although the model rocket mass was only 9.5 g, a model rocket was launched to 2 m. We confirmed the thrust generation [6]. In 2009, continuous thrust generation was obtained under multi-pulse operation [7] in a ground test. Subsequently, launch experiments were conducted under multi-pulse operations (Fig. 2 [8]). For launch experiments, the beam power, pulse duration, and pulse repetition frequency were, respectively, 600 kW, 1 ms, and 100 Hz. The 109 g model rocket consisted of a conical reflector and a cylindrical aluminum body without the air-breathing system. The respective diameter and length of the model rocket were 100 mm and 300 mm. As a result, the model rocket was launched to 1.2 m. However, when the beam transmission distance exceeded 2 m, the generated thrust was insufficient for launching because of the beam divergence [8]. In 2011, large thrust of 30 N was achieved using high power and high-frequency repetitive operation [9]. Table 1 presents results related to the thrust performance.

The achievement of 30 N thrust indicates that a kg class model rocket can be launched. Therefore, we set the next goal as a kg class model rocket launching to 10 m altitude.

Table 1 Thrust performance and operating conditions.

	2009	2011
Beam power @frequency	270 kW @50 Hz	570 kW @200 Hz
C_m	100 N/MW	360 N/MW
Time average thrust	2.3 N	30 N

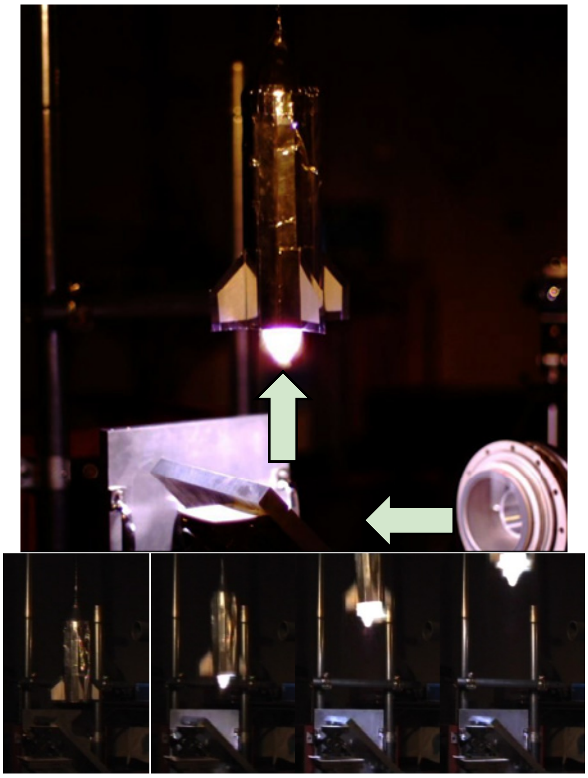

Fig. 2 The 109 g model rocket launch in a multi-pulse operation.

Long-distance millimeter-wave transfer is a key challenge. The transferred beam has a Gaussian profile. The beam radius ω is determined as

$$\omega = \omega_0 \left[1 + \left(\frac{z}{z_R}\right)^2\right]^{1/2} \tag{3}$$

where z stands for the transmission distance, ω_0 signifies the beam waist radius, and z_R denotes the Rayleigh length, defined as

$$z_R = \frac{\pi\omega^2}{2\lambda} \tag{4}$$

Here λ is the wavelength. When the transmission distance from the beam waist exceeds z_R, the beam radius began to expand; the diffraction loss increases. The transmission distance must equal twice the Rayleigh length to avoid diffraction loss.

Consequently, a millimeter-wave transfer system was developed as depicted in Fig. 3. The millimeter-wave beam generated by the 170 GHz high-power gyrotron was transmitted through the 63.5 mm corrugated waveguide. The transmission mirror system was composed of a couple of offset parabolic mirrors. It extended the beam radius from 20.4 to 120 mm. z_R was increased accordingly from 0.7 m to 25.7 m. A parabolic mirror with 280 mm-diameter and a 60 mm-diameter mirror were installed into the thruster to convert the beam profile and to guide it into the thruster tube. The incident beam power and pulse duration were 400 kW and 0.4 ms, respectively. Plasma was ignited in the thruster at 1 m, 3 m, and 5 m distance from the transmission mirror system. The time averaged thrust was measured from the thruster motion. As a result, 3.0 N thrust force was obtained at 100 Hz repetition frequency [8, 10].

A tapered-tube concentrator has also been proposed to receive the expanded beam. Fig. 4 shows that the concentrator directly connected to the model rocket and received the incident beam, guiding it into the model rocket. In high-power experiments, plasma ignition and ionization front propagation with the transmission system were confirmed when using incident power of 630 kW. Thrust generation was achieved [11, 12].

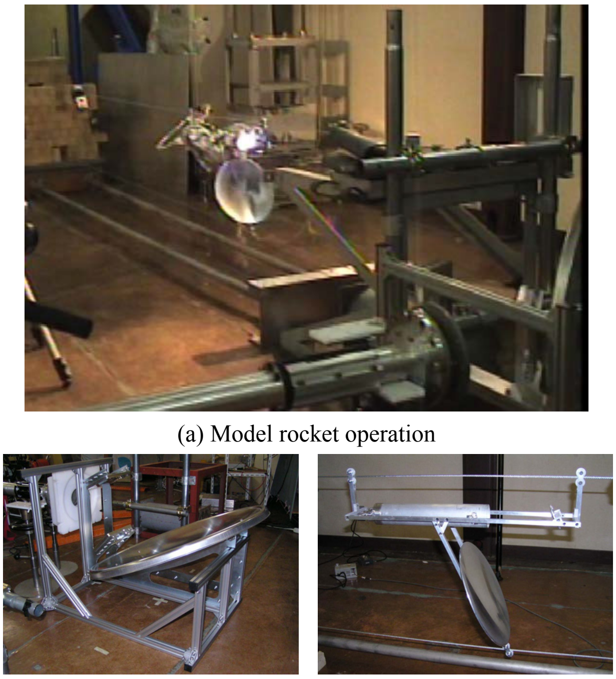

(a) Model rocket operation

(b) Transmission mirror system (c) Receiver mirror system

Fig. 3 Long-distance millimeter-wave transfer system with the receiving mirror system.

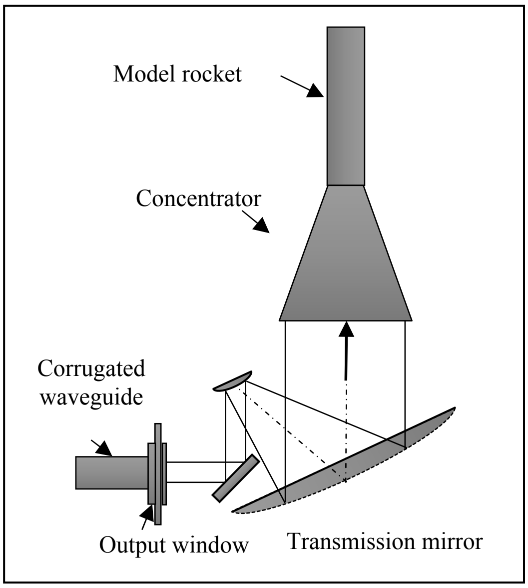

Fig. 4 Long-distance millimeter-wave transfer system with the tapered tube concentrator.

In multi-pulse operation, plasma remains even after the beam is turned off. Especially, in the concentrator where the beam radius and the plasma radius expand, the plasma remains for a long time: more than 10 ms. The discharge was ignited with the remaining plasma. Thrust generation was impeded because the plasma outside the thruster tube does not contribute to thrust generation. These abnormal ignitions also occur by the edges or internal structures of the thruster tube. Prevention or quenching of the abnormal ignitions will be examined as a challenge for future study.

4. Microwave Supported Detonation

Propagation of the ionization front absorbing the incident beam energy accompanying a shock wave is called detonation, as described above. If the incident beam is a laser, then the detonation is called LSD. Raizer et al. [13] have conducted pioneering studies in LSD. Several studies have examined LSD experimentally and computationally [14, 15 and references therein]. In MSD, Oda et al. [16-19] reported experimental observations using a high-speed camera at 170 GHz. Oda et al. had also measured the propagation velocity of the ionization front as a function of the incident beam power. The propagation velocity was found to be proportional with the incident power. Fig. 5 shows that the tendency is completely different from that of the LSD.

Actually, one can apply the detonation theory to the MSD only when the propagation velocity of the ionization front is the same as that of the shock wave. In the 170 GHz case, when the peak beam power density was lower than about 200 kW/cm^2, the propagation velocity of the shock wave was higher than that of the ionization front. The distance between the shock wave and ionization front then increases by time. From analogy of the chemical detonation theory, this condition is sometimes called MSC (microwave supported combustion). However, the condition is completely separate from combustion. The theory is inapplicable. In addition, the propagation velocity of the ionization front must be higher than that at the C-J condition.

In the one-dimensional stationary theory assuming that the control volume is fixed with the detonation front, the system of equations is described by the equation of continuity as

$$\rho_1 u_1 = \rho_2 u_2 \tag{5}$$

the equation of the momentum conservation,

$$p_1 + \rho_1 u_1^2 = p_2 + \rho_2 u_2^2 \tag{6}$$

the equation of the energy conservation,

$$\mathrm{C_p} T_1 + \frac{1}{2} u_1^2 + q = \mathrm{C_p} T_2 + \frac{1}{2} u_2^2 \tag{7}$$

and the equation of gas state,

$$p = \rho R T. \tag{8}$$

Here, C_p, p, R, T, u, q, and ρ respectively represent the specific heat at constant pressure, pressure, gas constant, temperature, flow velocity, absorbed energy per unit mass, and density. Indices 1 and 2 respectively denote conditions in front of the shock wave and behind the detonation. u_1 is the propagation velocity because the coordinate is fixed with the detonation. q is

$$q = \frac{\eta S_0}{\rho_1 u_1} \tag{9}$$

where, η is the absorption coefficient and S_0 is the beam power density.

The system of equations includes parameters p, T, ρ, u, and q. In the chemical detonation case, q is a constant determined by the fuel and equivalence ratio. However, in the case of MSD, the number of equations is insufficient to solve the system. Raizer et al. [13] have proposed a simple model for LSD assuming that the internal energy and pressure in front of the LSD are negligible compared with those behind the LSD. Shimada et al. [20] investigated the MSD condition at each propagation velocity fixing the absorbed energy. However, new equations for propagation velocity and absorption coefficient as a function of incident energy, beam frequency, gas pressure, and gas species are necessary to solve the system.

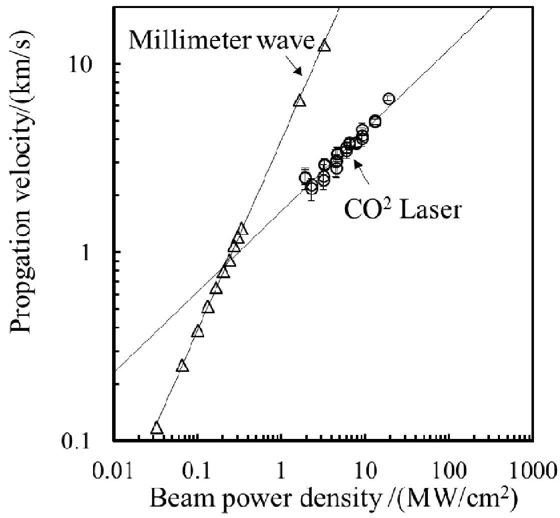

Fig. 5 Propagation velocities of the ionization front at respective beam power densities.

5. Millimeter Wave Discharge Structure

In the time-integral image of the MSD, fine filament structures can be observed. This structure is self-organized and determined by nonlinear dynamics.

Discharge at the microwave frequency band has been studied since 1940. The fundamental physics has been clarified. However, the discharge in millimeter wave frequency band has recently become available because of gyrotron development. Early experiments examining this discharge using a gyrotron were conducted in the 1980s. Vikharev et al. [21] reported the pressure dependence of helium and nitrogen gas discharge generated by a focused 37.5 GHz millimeter wave (λ = 8 mm wavelength). Hidaka et al. [22] investigated the evolution of the filament using a mirror to focus 110 GHz millimeter wave beams; they asserted that filaments are generated by a standing wave.

A millimeter-wave discharge can be categorized as either sub-critical or overcritical depending on the incident beam power density. In the overcritical region, the incident beam power density closes to the ionization threshold of the gas. A standing-wave generated by the incident and a reflected beam from the ionization front contribute to the structure. The local beam power density at the standing wave exceeds the ionization threshold, resulting in new filament ignition. The process occurs repeatedly along the beam pulse width. Consequently, the ionization front propagates toward the beam source. The propagation velocity was measured as 10^5 m/s to 10^4 m/s in Hidaka's experiment. The pitch of each filament is slightly shorter than one-quarter of the wavelength (λ/4 structure) because of the skin depth of the plasma. The discharge also stretches along the electric field of the incident beam. Consequently, in the (***E***, ***k***) plane, which contains the wave vector ***k*** parallel to the electric field vector ***E***, a filament array is generated, whereas a lattice-like pattern appeared in the (***H***, ***k***) plane, which contains ***k*** parallel to the magnetic field vector ***H***. The overcritical condition has been reproduced numerically by Bouef et al. [23], who calculated the electromagnetic field using the FDTD (finite-difference time-domain) method and induced the electron number density n_e by the diffusion equation of

$$\frac{\partial n_e}{\partial t} - D_{\mathrm{eff}}\Delta n_e = v_{\mathrm{eff}} n_{\mathrm{e}} \quad (10)$$

where,

$$v_{\mathrm{eff}} = v_a\left[\left(\frac{E_{\mathrm{eff}}}{E_c}\right)^{\beta} - 1\right] \quad (11)$$

And v_a signifies the attachment frequency, E_c denotes the critical intensity, E_{eff} is the local effective electric field intensity, D_{eff} represents the effective diffusion coefficient, and β stands for a numerical constant.

The millimeter-wave discharge in the MSD is expected to be in the sub-critical condition, for which the incident beam power density is much lower than the ionization threshold. The ionization front cannot jump. Therefore, the λ/4 is not formed. Instead, granular plasmas propagate toward the beam source. The trajectories form stream lines, also known as filaments, in the time-integral image (Fig. 6). The typical propagation velocity is 10^2 m/s. Few studies have examined the sub-critical condition. Oda's experiments contributed to the sub-critical condition, as described above. Bratman et al. [24] reported the discharge at 0.55 THz. Experiments conducted by Bogatov et al. [25] might account for the sub-critical.

VoskoboÏnikova et al. pointed out that, in the sub-critical condition, the time scale of the discharge evolution is comparable to the gas-dynamics process. In addition, reduction of the gas (neutral particle) density in the discharge because of Joule heating contributes to the ionization process [26]. They reproduced spark streamer discharges in the subcritical region. The absolute value of the local electric field intensity divided by the number density of the gas $|E|/n$ was calculated. When $|E|/n$ exceeds the critical value $(|E|/n)_{\mathrm{c}}$ at the streamer head, the number of electrons increases because of the ionization.

Takahashi et al. [27] calculated the discharge and deduced the thrust performance at respective pressures. Takahashi et al. also proposed the use of ECH (electron cyclotron heating) on-board an external

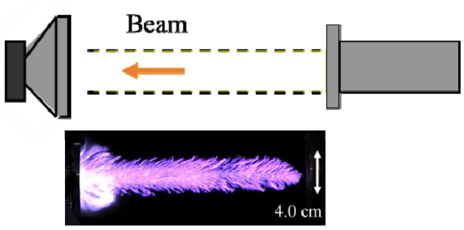

Fig. 6 Experimental setup and images of the filament structure.

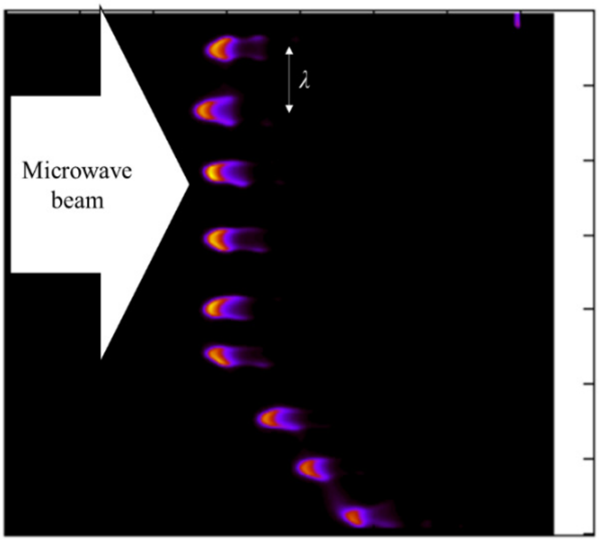

Fig. 7 Numerical computation result of the number density of the electron.

magnet. They showed a drastic increase in the thruster performance using ECH [27].

Reconsidering the ionization model in the source term presents another challenge. Fig. 7 depicts a numerical computation result. The source term was modified artificially. The propagation of granular plasma was reproduced [28].

6. Microwave Rocket Feasibility Studies

Thrust generation and multi-pulse operation have already been demonstrated through launch experiments. From these launch experiments, the momentum coupling coefficient of Microwave Rockets is expected to be close to 300 N/MW. Assuming beam power of 1 MW and a duty cycle of 0.2 for the millimeter wave beam pulse, the Microwave Rocket acquires the time average thrust of 60 N. In actual flight, millimeter wave attenuation by atmospheric air

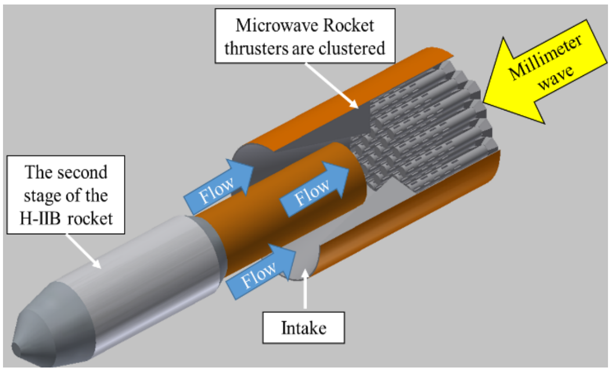

Fig. 8 Schematic image of the Japanese H-IIB replaced the first stage engine and solid rocket boosters by the Microwave Rocket.

and a decrease in air density affects the thrust performance. Consequently, the Microwave Rocket launch capability is expected to be 1-2 kg/MW.

Some Microwave Rocket feasibility studies have been done. For a case in which the first stage engine and solid rocket boosters of Japanese H-IIB are replaced by a Microwave Rocket, the payload ratio is expected to be increased from 3.45% to 15.5%. Fig. 8 portrays the model rocket. The total mass was reduced from 531 tons to 122.2 tons. The required beam power was estimated as 188 GW to carry a 19 tons payload to LEO. The resulting launch cost per unit payload becomes lower than that of a conventional H-IIB at about 20 launches. At one thousand launches, the construction cost of the beam facility becomes fully amortized. The cost reduction reached 77% in the analysis [29].

Kakinuma et al. [31] proposed a TSTO (two-stage-to-orbit transporting) launch system with a Microwave Rocket first stage and a Microwave Thermal Rocket second stage, as proposed by Parkin et al. [30]. The wet mass of the whole rocket was assumed as 50 kg. For the first stage task, the Microwave Rocket brings a Microwave Thermal Rocket to a high altitude instead of the UAV (unmanned aerial vehicle). The Microwave Rocket is simpler, faster, and reaches a higher altitude at higher speed. Additionally, they presented a new trajectory that eliminates power beaming at low elevation angles, which improves system performance. The whole launch system has remarkable performance of a three times larger payload fraction. The launch cost per unit mass of payload is only one quarter that of the case of the UAV. These differences are expected to be much more pronounced in a larger scale launch system. As a result, to demonstrate an 8 kg satellite launch, beam facility construction cost of $490 M, vehicle cost of $46 k, and electricity cost of $150 were expected [31].

7. Conclusions

Microwave Rockets are promising candidates as breakthroughs to reduce mass transportation costs to the space drastically. However, numerous challenges remain, which include the physics of MSD and its application to thrust performance optimization, air-breathing systems (which are not described herein), long-distance beam power transportation, and abnormal ignition. In addition, feasibility studies indicate a huge initial cost for ground facilities. Nevertheless the cost estimations might be optimistic. Although the construction costs can be amortized, reduction of costs will be necessary, especially in early stages. Furthermore, one must consider regulations of radio use in Japan. Currently, of course, no frequency band is allowed to irradiate such a high power beam externally. These are reasons why the Microwave Rocket remains interesting as a challenge for future research efforts.

Acknowledgements

This work was supported by a Grant-in-Aid for Scientific Research (S), No. 15H05770.

References

[1] Kantrowitz, A. 1972. "Astronaut." *Aeronaut* 10: 74-6.

[2] Phipps, C., Birkan, M., Bohn, W., Eckel, H.-A., Horisawa, H., Lippert, T., Michaelis, M., Rezunkov, Y., Sasoh, A., Schall, W., Scharring, S., and Sinko, J. 2010. "Review: Laser-Ablation Propulsion." *Journal of Propulsion and Power* 26 (4): 609-37.

[3] Komurasaki, K., and Wang, B. 2010. *Encyclopedia of Aerospace Engineering*. Hoboken: John Wiley & Sons Ltd., 1351.

[4] Myrabo, L. 2001. "World Record Flight of Beam-Riding Rocket Lightcraft: Demonstration of 'Disruptive' Propulsion Technology." In *Proceedings of the 37th AIAA/ASME/SAE/ASEE Joint Propulsion Conference,* Salt Lake City, US.

[5] Sakamoto, K., Kasugai, A., Takahashi, K., Minami, R., Kobayashi, N., and Kajiwara, K. 2007. "Achievement of Robust High-efficiency 1|[thinsp]|MW Oscillation in the Hard-Self-Excitation Region by a 170|[thinsp]|GHz Continuous-wave Gyrotron." *Nature Physics* 3 (6): 411-4.

[6] Nakagawa, T., Mihara, Y., Komurasaki, K., Takahashi, K., Sakamoto, K., and Imai, T. 2004. "Propulsive Impulse Measurement of a Microwave-Boosted Vehicle in the Atmosphere." *Journal of Spacecraft and Rockets* 41 (1): 151-3.

[7] Oda, Y., Shibata, T., Komurasaki, K., Takahashi, K., Kasugai, A., and Sakamoto, K. 2009. "Thrust Performance of Microwave Rocket under Repetitive-Pulse Operation." *Journal of Propulsion and Power* 25 (1): 118-22.

[8] Yamaguchi, T., Komurasaki, K., Oda, Y., Kajiwara, K., Takahashi, K., and Sakamoto, K. 2011. "Millimeter-Wave Beam Conversion with Quasi-Optical Mirrors for Microwave Rocket Launch Demonstration." *AIP Conference Proceedings* 1402 (1): 467-77.

[9] Komatsu, R., Yamaguchi, T., Oda, Y., Saitoh, S., Fukunari, M., Komurasaki, K., Kajiwara, K., Takahashi, K., and Sakamoto, K. 2012. "Thrust Augmentation of Microwave Rocket with High-Power and High-Duty-Cycle Operation." *Journal of the Japan Society for Aeronautical and Space Science* 60 (6): 235-7 (in Japanese).

[10] Oda, Y., Yamaguchi, T., Shimada, Y., Komurasaki, K., Kajiwara, K., Takahashi, K., and Sakamoto, K. 2010. "Study of High-Power Millimeter-Wave Beam Transmission for Microwave Beaming Propulsion." In *Proceedings of the 35th International Conference on Infrared, Millimter, and Terahertz Waves*, Rome, Italy.

[11] Fukunari, M., Wongsuryrat, N., Yamaguchi, T., Nakamura, Y., Komurasaki, K., and Koizumi, H. 2017. "Design of a Millimeter-Wave Concentrator for Beam Reception in High-Power Wireless Power Transfer." *Journal of Infrared, Millimeter, and Terahertz Waves* 38 (2): 176-90.

[12] Fukunari, M., Yamaguchi, T., Saitoh, S., Asai, K., Kurita, S., Komurasaki, K., Oda, Y., Kajiwara, K., Takahashi, K., and Sakamoto, K. 2013. "Thrust Performance and Plasma Generation of Microwave Rocket with Microwave Beam Space Transmission System." In *Proceedings of the IEEE Pulsed Power & Plasma Science Conference*, San Francisco, California, USA.

[13] Raizer, Y. P. 1965. "Breakdown and Heating of Gases with a Laser Light Pulse." *Sov. Phys. JETP* 21 (5): 1009-17.

[14] Shimamura, K., Matsui, K., Ofosu, J. A., Yokota, I., and Komurasaki, K. 2017. "Mode Transition of Plasma Expansion for Laser Induced Breakdown in Air." *Applied Physics Letters* 110: 134104.

[15] Mori, K., Komurasaki, K., and Arakawa, Y. 2006. "Threshold Laser Power Density for Regime Transition of a Laser Absorption Wave in a Reduced-Density Air Atmosphere." *Applied Physics Letters* 88 (12): 59-104.

[16] Oda, Y., Komurasaki, K., Kasugai, A., and Sakamoto, K. 2006. "Plasma Generation Using High-Power Millimeter-Wave Beam and Its Application for Thrust Generation." *Journal of Applied Physics* 100 (11): 32-156.

[17] Oda, Y., Komurasaki, K., Takahashi, K., Kasugai, A., Imai, T., and Sakamoto, K. 2007. "Plasma Generation at Atmospheric Pressure Using a High-Power Microwave Beam and Its Application to Rocket Propulsion." *Electrical Engineering in Japan* 161 (2): 1-7.

[18] Oda, Y., Yamaguchi, T., Shiraishi, Y., Komurasaki, K., Kajiwara, K., Takahashi, K., Kasugai, A., and Sakamoto, K. 2011. "A One-Dimensional Propagation of Shock Wave Supported by Atmospheric Millimeter-Wave Plasma." *Journal of Infrared, Millimeter and Terahertz Waves* 32 (6): 877-82.

[19] Oda, Y., Kajiwara, K., Takahashi, K., Kasugai, A., and Sakamoto, K. 2008. "Development of Filamentary Structure of Atmospheric Breakdown on 170 GHz Gaussian Beam." In *Proceedings of the IEEE 35th International Conference on Plasma Science*, Karlsruhe, Germany.

[20] Shimada, Y., Shibata, T., Yamaguchi, T., Oda, Y., Kajiwara, K., Takahashi, K., Kasugai, A., Sakamoto, K., Komurasaki, K., and Arakawab, Y. 2010. "Propagating Structure of a Microwave Driven Shock Wave Inside a Tube." *AIP Conference Proceedings* 1230 (1): 366-76.

[21] Vikharev, L., Gil'denburg, V. B., Golubev, S. V., Eremin, B. G., Ivanov, O. A., Litvak, A. G., Stepanov, A. N., and Yunakovskii, A. D. 1988. "Nonlinear Dynamics of a Freely Localized Microwave Discharge in an Electromagnetic Wave Beam." *Sov. Phys. JETP* 67 (4): 724-8.

[22] Hidaka, Y., Choi, E. M., Mastovsky, I., Shapiro, M. A., Sirigiri, J. R., and Temkin, R. J. 2008. "Observation of Large Arrays of Plasma Filaments in Air Breakdown by 1.5-MW 110-GHz Gyrotron Pulses." *Physical Review Letters* 100 (3): 035003.

[23] Boeuf, J. P., Chaudhury, B., and Zhu, G. Q. 2010. "Theory and Modeling of Self-organization and Propagation of Filamentary Plasma Arrays in Microwave Breakdown at Atmospheric Pressure." *Physical Review Letters* 104 (1): 015002.

[24] Bratman, V. L., Zorin, V. G., Kalynov, Y. K., Koldanov, V. A., Litvak, A. G., Razin, S. V., Sidorov, A. V., and Skalyga, V. A. 2011. "Plasma Creation by Terahertz Electromagnetic Radiation." *Physics of Plasma* 18 (8): 083507.

[25] Bogatov, N. A., Bykov, Y. V., Venediktov, N. P., Goludev, S. V., Zorin, V. G., Eremeev, A. G., and Semenov, V. E. 1986. "Gasdynamic Propagation of a Nonequiliburium Micorwave Discharge." *Soviet Journal of Plasma Physics* 12 (6): 416-20.

[26] VoskoboÏnikova, O. I., Ginzburg, S. L., D'yachenko, V. F., and Khodataev, K. V. 2002. "Numerical Investigation of Subcritical Microwave Discharges in a High-Pressure Gas." *Technical Physics* 47 (8): 955-60.

[27] Takahashi, M., and Ohnishi, N. 2016. "Plasma Filamentation and Shock Wave Enhancement in Microwave Rockets by Combining Low-Frequency Microwaves with External Magnetic Field." *Journal of Applied Physics* 120 (6): 40-2.

[28] Nakamura, Y., Fukunari, M., Yamaguchi, T., Komurasaki, K., and Koizumi, H. 2016. "Numerical Analysis of Comb Shaped Plasma Front Propagation in Millimeter-Wave Discharge under Atmospheric Pressure." In *Proceedings of the 47th AIAA Plasma Dynamics and Lasers Conference, AIAA Aviation and Aeronautics Forum and Exposition*, Washington, DC, US.

[29] Fukunari, M., Arnault, A., Yamaguchi, T., and Komurasaki, K. 2014. "Replacement of Chemical Rocket Launchers by Beamed Energy Propulsion." *Applied Optics* 53 (31): I16-22.

[30] Parkin, K. L. G., Didomenico, L., and Culick, F. C. 2004. "The Microwave Thermal Thruster Concept." *2nd International Symposium on Beamed Energy Propulsion* 702 (1): 418.

[31] Kakinuma, K., Fukunari, M., Yamaguchi, T., Nakamura, Y., Koizumi, H., Komurasaki, K., and Parkin, K. 2016. "Two-Stage-to-Orbit Transporting System Combining Microwave Rocket and Microwave Thermal Rocket for Small Satellite Launch." *Aerospace Technology Japan* 14: 99-103.